CHINESE JOURNAL OF PHYSICS VOL. 52, NO. 1-I February 2014

A Theoretical Analysis of Zero Field Splitting Parameters of Mn^{2+} Doped Diglycine Calcium Chloride Tetrahydrate

Sangita Pandey* and Ram Kripal†

EPR laboratory, Department of Physics,
University of Allahabad, Allahabad (India)-211002
(Received March 26, 2013; Revised June 8, 2013)

The crystal field parameters (CFPs) of Mn^{2+} in Diglycine calcium chloride tetrahydrate (DGCCT) are calculated using the superposition model. The zero field splitting parameters (ZFSPs) D and E are then evaluated using perturbation and microscopic spin Hamiltonian (SH) theory. The calculated second-rank axial and rhombic ZFSPs are compared with the experimental ones. Both the ZFSPs D and E evaluated theoretically are in good agreement with the experimental values obtained by electron paramagnetic resonance. The results suggest that the Mn^{2+} ion occupies the Ca^{2+} substitutional site in DGCCT.

DOI: 10.6122/CJP.52.262 PACS numbers: 71.70.Ch, 76.30.-v, 76.30.Fc, 78.20.Ci

I. INTRODUCTION

The superposition model was developed to find physical and geometrical information existing in the crystal field parameters [1, 2]. The first extension of this model to 'exotic' forms of the crystal field is done, where two-electron or correlation crystal field effects are examined. A second extension to the 'vector' crystal field describing transition intensities is also done. The positions of various ligands are required in applying this model. Hence the relation between the model and the theories of local distortion in crystals is of potential interest. The EPR spectrum of Fe^{3+} has been used to probe the structural phase transitions of $BaTiO_3$. Siegel and Müller [3] used a one-parameter model to describe the position of the Fe^{3+} ion relative to the surrounding oxygen octahedron, which is assumed to be undisturbed by the substitution. Yeung [4] analyzed the Mn^{2+} spin Hamiltonian parameters using this model with an allowance for local distortion and obtained quite reasonable results.

Theoretical studies on the spin Hamiltonian parameters of d^5 ions have become the subject of interest of many workers [5–14]. The lack of orbital angular momentum in the ^6S ground state leads to considerable difficulty in explaining the observed effects of the crystal field. Different mechanisms were suggested to contribute to the ground state splitting of the magnetic ions incorporated in the lattices [15]. The effect of the spin Hamiltonian mechanism may be considered by perturbation procedures. In the mostly used perturbation procedure, the cubic field and the diagonal part of the free-ion Hamiltonian are taken as

*Electronic address: sangitapandey2009@gmail.com
†Electronic address: ram_kripal2001@rediffmail.com

unperturbed terms, while the spin-orbit coupling, the low-symmetry field, and the off-diagonal part of the free-ion Hamiltonian are considered as the perturbation terms [16].

Electron paramagnetic resonance (EPR) studies of Mn^{2+} doped Diglycine calcium chloride tetrahydrate (DGCCT) single crystals have been reported [17]. There are two possibilities for the Mn^{2+} site in the DGCCT crystal, namely substitutional and interstitial. It is interesting to investigate the site of this impurity. It was found [17] that Mn^{2+} ion enters the lattice substitutionally at the Ca^{2+} site. In the present study, the axial and rhombic zero-field splitting parameters (ZFSPs) are calculated for the Mn^{2+} ion present at the substitutional Ca^{2+} site in DGCCT, using crystal field parameters (CFPs) from the superposition model and perturbation expressions [18]. The result derived from this model is in agreement with the experimental observations.

II. CRYSTAL STRUCTURE

The DGCCT single crystals are monoclinic, space group $P2_1/n$ with Z = 4 [19]. The unit cell dimensions are $a = 1.301$ nm, $b = 0.679$ nm, $c = 1.538$ nm, and $\beta = 91.4^\circ$ [17]. The Ca atom is coordinated to seven O atoms, three of them belonging to water molecules and the remaining four belonging to the carboxyl groups of the glycine molecules (Fig. 1).

III. THEORETICAL INVESTIGATION

The experimental resonance fields are analyzed using the spin Hamiltonian [20, 21]

$$\begin{aligned}\mathcal{H} \;=\; & g\mu_B \mathbf{B}.\mathbf{S} + \mathrm{D}\left\{S_z^2 - \frac{1}{3}S(S+1)\right\} + \mathrm{E}\left(S_x^2 - S_y^2\right) \\ & + \left(\frac{a}{6}\right)\left[S_x^4 + S_y^4 + S_z^4 - \frac{1}{5}S(S+1)(3S^2+3S-1)\right] \\ & + \frac{F}{180}\left\{35S_z^4 - 30S(S+1)S_z^2 + 25S_z^2 - 6S(S+1) + 3S^2(S+1)^2\right\} \\ & + \frac{K}{4}\left[\left\{7S_z^2 - S(S+1) - 5\right\}\left(S_+^2 + S_-^2\right) + \left(S_+^2 + S_-^2\right)\left\{7S_z^2 - S(S+1) - 5\right\}\right] \\ & + AS_zI_z + B\left(S_xI_x + S_yI_y\right), \end{aligned} \tag{1}$$

where g is the isotropic spectroscopic splitting factor, μ_B the Bohr magneton, and B the external magnetic field. The parameters D and E are the second-rank axial and rhombic ZFSPs, whereas a, F, and K are the fourth-rank cubic, axial, and rhombic ones, respectively. The last two terms in Eq. (1) represent the hyperfine ($I = 5/2$) interaction. The F and K terms are deleted here as their effect is small [20, 22, 23]. The isotropic approximation used for the electronic Zeeman interaction is generally valid for $3d^5$ ions [20, 24]. The two approximations in question may slightly affect the fitted value of a [25]. The direction of the maximum overall splitting of the EPR spectrum is taken as the z-axis and that of the minimum as the x-axis [26]. The laboratory axes (x, y, z) determined from the EPR

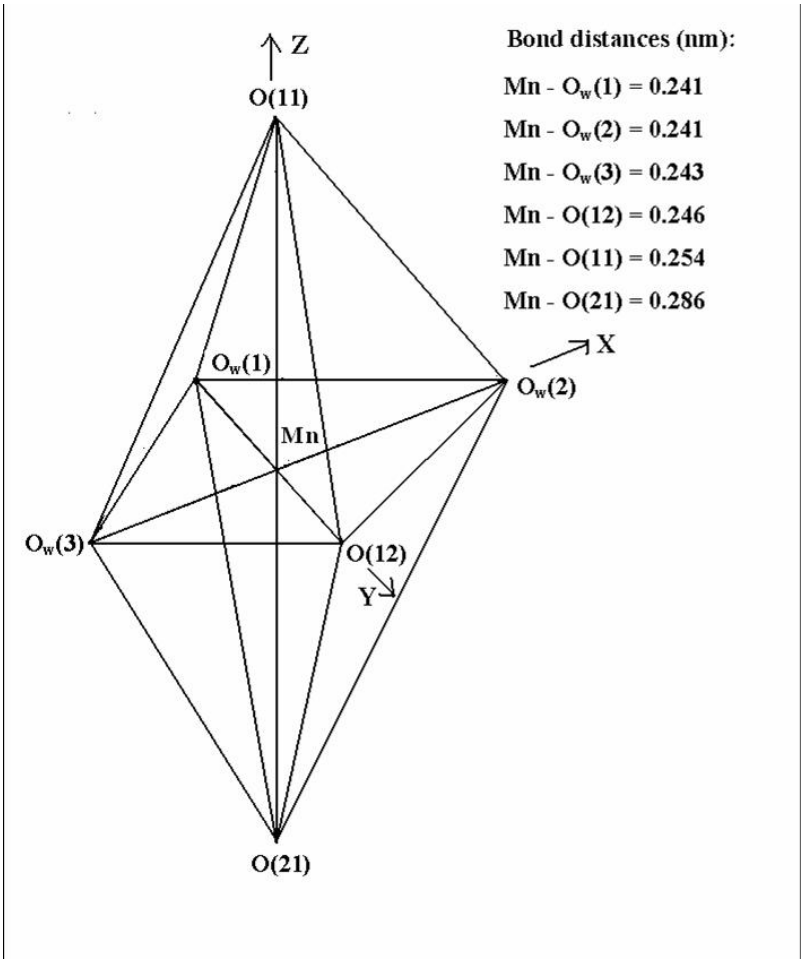

FIG. 1: Coordination around Mn^{2+} in a DGCCT single crystal.

spectra are found to coincide with the crystallographic axes (CA). The z-axis of the local site symmetry axes, i.e., the symmetry adapted axes (SAA) is along the metal oxygen bond and the other two axes (x, y) are perpendicular to the z-axis.

In DGCCT, the calcium ion is located within a distorted octahedron of oxygen ions [19], and the local symmetry is approximately orthorhombic of the first kind (OR-I) [27]. In an OR-I symmetry, the SO contributions to the ZFSPs D and E of the $3d^5$ ions were derived [18, 28] as

$$D^{(4)}(SO) = (3\xi^2/70P^2D)(-B_{20}^2 - 21\xi B_{20} + 2B_{22}^2) + (\xi^2/63P^2G)(-5B_{40}^2 - 4B_{42}^2 + 14B_{44}^2), \quad (2)$$

$$E^{(4)}(SO) = (\sqrt{6}\xi^2/70P^2D)(2B_{20} - 21\xi)B_{22} + (\xi^2/63P^2G)(3\sqrt{10}B_{40} + 2\sqrt{7}B_{44})B_{42}, \quad (3)$$

where P = 7B + 7C, G = 10B + 5C, and D = 17B + 5C; B and C are the Racah parameters. Only the fourth order term is considered here as the first-, second-, third-, fifth-, and sixth-

order perturbations of D and E are zero [18]. Eqs. (2) and (3) are appropriate for weak-field cases, and are still correct even when the low-symmetry components are comparable with the cubic part [18].

By considering the covalency effect via the average covalency parameter N, the B, C, and ξ can be expressed in terms of N as [29, 30]

$$\mathrm{B}{=}\mathrm{N}^4\mathrm{B}_0, \qquad \mathrm{C}{=}\mathrm{N}^4\mathrm{C}_0, \qquad \xi_\mathrm{d} {=}\mathrm{N}^2\xi_d^0, \tag{4}$$

where B_0 and C_0, and ξ_d^0 denote the free ion Racah and the spin-orbit coupling parameters, respectively [29, 30]. The following values of B_0 and C_0 and ξ_d^0 for the free Mn^{2+} ion are used: $\mathrm{B}_0 = 960\ \mathrm{cm}^{-1}$, $\mathrm{C}_0 = 3325\ \mathrm{cm}^{-1}$, $\xi_d^0 = 335\ \mathrm{cm}^{-1}$ [20].

From optical absorption study [17]: $\mathrm{B} = 770\ \mathrm{cm}^{-1}$ and $\mathrm{C} = 2322\ \mathrm{cm}^{-1}$ were obtained. Eq. (4) yields N = 0.946 and N = 0.914, respectively. The average value [30] of $\mathrm{N} = (\sqrt{B/B_0} + \sqrt{C/C_0})/2 = 0.86$ is used to calculate the ZFSPs D and E from Eqs. (2) and (3).

The superposition model is used to calculate the CFPs, B_{kq} for the Mn^{2+} ion in a DGCCT single crystal, and ZFSPs are then calculated using these B_{kq} parameters.

The superposition model has been shown to be quite successful in explaining the crystal-field splitting of the $4f^n$ ions [31] and recently of some $3d^n$ ions [32–34]. The superposition model expresses the CFPs as [18, 31]

$$\mathrm{B}_{kq} = \sum \overline{A_k}(R_j)\mathrm{K}_{kq}(\theta_j, \phi_j). \tag{5}$$

In this equation the various symbols have the following meanings: R_j are the distances between the paramagnetic ion Mn^{2+} and the ligand ion j, R_0 is the reference distance, normally chosen near a value of the R_js. θ_j are the bond angles in a chosen axis system (preferably the symmetry adapted axes system (SAAS)) [35, 36]. Summation is taken over all the nearest neighbour ligands. The coordination factor K_{kq} (θ_j, ϕ_j) are explicit functions of the angular position of the ligand [18, 35, 37, 38]. The intrinsic parameter $\overline{A_k}(R_j)$ is given by the power law [16, 27]:

$$\overline{A_k}(R_j) = \overline{A_k}(R_0)(R_0/R_j)^{\mathrm{t}_k}, \tag{6}$$

where $\overline{A_k}$ (R_0) is an intrinsic parameter for a given ion host system. The symbol t_k is the power law exponent. The crystal-field parameters B_{kq} can be obtained using the superposition model given by Eq. (5) and are given in Appendix A [39].

For $3d^5$ ions, $\overline{A_2}(R_0)/\overline{A_4}(R_0)$ is 8–12 [5, 33]. In the present study, we have taken $\overline{A_2}(R_0)/\overline{A_4}(R_0) = 10$. For $3d^N$ ions in the 6-fold cubic coordination $\overline{A_4}(R_0)$ can be found from the relation $\overline{A_4}(R_0) = (3/4)$ Dq [18]. As $\overline{A_4}(R_0)$ is independent of the coordination [40], we have used the above relation to determine $\overline{A_4}(R_0)$ in our calculation using Dq $= 716\ \mathrm{cm}^{-1}$ [17]. The values of R_1, R_1', R_2, R_2', R_3, R_3'; θ_1, θ_1', θ_2, θ_2', θ_3, θ_3'; ϕ_1, ϕ_1', ϕ_2, ϕ_2', ϕ_3, and ϕ_3' used in the calculation are: 0.238 nm, 0.239 nm, 0.245 nm, 0.248 nm, 0.253 nm, 0.287 nm; 93.4°, 92.3°, 86.4°, 87.9°, 0°, 180°; 0°, 90°, 180°, 270°, 0°, and 0°, respectively.

IV. RESULT AND DISCUSSION

At first to check the substitution at the Ca^{2+} site, the origin of Mn^{2+} was shifted at the Ca^{2+} ion. Since the ionic radius of the impurity Mn^{2+} ion (0.080 nm) is much smaller than that of the host Ca^{2+} (0.114 nm), an off-center displacement can be expected [41]. Taking $\Delta z = 0.002$ and $\Delta y = 0.001$, the coordinates x, y, z and bond distances of different ligands, R_j as well as the angles θ_j and ϕ_j were calculated and are given in Table I. While adjusting the Mn-O distances to match the experimental result, it is kept in mind that the site symmetry is preserved as well as the energy is minimized, and thus the structural stability is taken into account. Taking R_0 as the minimum of R_j [42], i.e., $R_0 = 0.238$ nm, $\overline{A_2}(R_0)/\overline{A_4}(R_0) = 10$, $t_2 = 3$, $t_4 = 7$ [5], we obtain D and E to be 99×10^{-4} cm^{-1} and 12×10^{-4} cm^{-1}, respectively, which are inconsistent with the experimental values. We have then calculated D and E taking the average value of the metal-oxygen distances as R_0 [43], i.e., $R_0 = 0.252$ nm and the other parameters as above, which come out to be 285×10^{-4} cm^{-1} and 33×10^{-4} cm^{-1}, respectively. These values of D and E are also not in good agreement with the experimental values. Therefore, we have calculated D and E without considering an off-center displacement. The bond distances of different ligands R_j and the angles θ_j and ϕ_j calculated for this case are given in Table II. Taking R_0 as the average of R_j [42], i.e., $R_0 = 0.252$ nm, $\overline{A_2}(R_0)/\overline{A_4}(R_0) = 10$, $t_2 = 3$, $t_4 = 7$ [5]; we obtain D and E to be 373×10^{-4} cm^{-1} and 40×10^{-4} cm^{-1}, respectively, which are inconsistent with the experimental values. We have then calculated D and E taking the lowest value of the metal-oxygen distances as R_0 [42], i.e., $R_0 = 0.241$ nm and the other parameters as above, which come out to be 163×10^{-4} cm^{-1} and 19×10^{-4} cm^{-1}, respectively. These values are also inconsistent with the experimental values. Further, we have calculated D and E taking $R_0 = 0.252$ nm, $\overline{A_2}(R_0)/\overline{A_4}(R_0) = 12$, $t_2 = 4$, $t_4 = 6$ and obtain these values to be 260×10^{-4} cm^{-1} and 34×10^{-4} cm^{-1}, respectively, which are smaller and also inconsistent with the experimental values. Therefore, we have taken $R_0 = 0.252$ nm [5], $\overline{A_2}(R_0)/\overline{A_4}(R_0) = 11$, $t_2 = 6$, $t_4 = 7$. This provides D and E data (Table III) which are in good agreement with the experimental values. Such model calculations by changing the SPM parameters t_2 and t_4 have been done earlier in the case of Mn^{2+} and Fe^{3+} doped anatase TiO_2 crystal [44]. Therefore, we can say that Mn^{2+} ion substitutes for the Ca^{2+} ion (without an off-center displacement). In this way, the conclusion drawn on the basis of the superposition model supports the experimental result that the Mn^{2+} ions take up a substitutional Ca^{2+} site in the crystal [17]. For comparison we have also investigated the interstitial sites for Mn^{2+} ions. The predicted values of ZFSPs come out to be considerably larger than the experimental ones, and hence we are not giving the full results here.

The calculated values of the B_{kq} parameters using Eq. (5) and the S5 transformation [25, 26] are obtained (in cm^{-1}) as: $B_{20} = 7202.34$, $B_{22} = 180.02$, $B_{40} = 868.51$, $B_{42} = 5503.36$, and $B_{44} = 10742.35$. The ratio $B_{22}/B_{20} = 0.025$, which indicates that the CFPs are standardized [25, 26].

The calculated ZFSPs for the Mn^{2+} ion in DGCCT crystal using Eqs. (2), (3) and the CFPs from the superposition model are given in Table III. The experimental values are also shown here for comparison. The calculated values of the ZFSPs are in reasonable

TABLE I: Coordinates of oxygen ligands, Mn-oxygen bond distances R_j, and coordination angles θ_j and ϕ_j for Mn^{2+} ion doped DGCCT single crystals (when the Mn^{2+} ion is assumed to be at the Ca^{2+} site with an off-center displacement).

Oxygen Ligands	x	y	z	Mn-oxygen bond distance R_j (nm)	Angle θ_j (Degree)	Angle ϕ_j (Degree)
$O_w(2)$	0.0615	0.0841	−0.1397	0.238	93.4	0
$O_w(1)$	−0.1465	0.0411	−0.0957	0.239	92.3	90
$O_w(3)$	0.0565	−0.0189	0.1533	0.245	86.4	180
O(12)	−0.1555	−0.0409	0.0883	0.248	87.9	270
O(11)	0.1765	−0.1559	−0.0087	0.253	0	0
O(21)	0.2025	0.1611	0.0233	0.287	180	0

TABLE II: Metal-oxygen bond distances R_j and coordination angles θ_j and ϕ_j for Mn^{2+} ion doped DGCCT single crystals (when the Mn^{2+} ion is assumed to be at the Ca^{2+} site without an off-center displacement).

Metal-oxygen	Metal-oxygen bond distance R_j (nm)	Angle θ_j (Degree)	Angle ϕ_j (Degree)
Mn-$O_w(2)$	0.241	93.4	0
Mn-$O_w(1)$	0.241	92.3	90
Mn-$O_w(3)$	0.243	86.4	180
Mn-O(12)	0.246	87.9	270
Mn-O(11)	0.254	0	0
Mn-O(21)	0.286	180	0

agreement with the values obtained from the experiment [17]. Using the above B_{kq} parameters and the CFA program [45] and considering the OR-I symmetry of the crystal field the optical spectra of Mn^2 doped DGCCT crystals are calculated. The CFA program allows for finding the complete energy level scheme for any $3d^N$ ion in a crystal field of arbitrarily low symmetry within the whole basis of $3d^N$ states. The energy levels of the impurity ion are obtained by diagonalization of the complete Hamiltonian within the $3d^N$ basis of states in the intermediate crystal field coupling scheme. The calculated energy values are given in Table IV along with the experimental ones for comparison. There is a reasonable agreement between these two. This indicates that the Mn^{2+} ion is occupying the substitutional site in a DGCCT single crystal. Thus, our calculation based on the superposition model supports the experimental results reported earlier [17]. The calculated results are compared to the EPR and optical absorption data at 77 and 300 K, respectively. The calculated results

TABLE III: Comparison of the ZFSPs calculated by the superposition model for the Mn^{2+} ion doped DGCCT single crystal with the experimental values.

	Values of ZFSPs ($\times 10^{-4}$ cm^{-1})	
	|D|	|E|
Calculated	288	58
Experimental	276	58

match equally well at 77 and 300 K, perhaps due to no change in the structure of the crystal at both the temperatures. On cooling the crystal to 77 K from 300 K, the fine structure of the bands becomes clear, and the bands show some shift in position due to the effects of the spin-orbit and vibrational interactions. The parameters B, C and Dq also change slightly. In the case of $RbMnF_3$ [46], the shift of the various bands of Mn^{2+} ranges from 23 to 335 cm^{-1} in going to 77 K from 300 K. B, C, Dq become B = 840 cm^{-1}, C = 3080 cm^{-1}, Dq = 780 cm^{-1} at 77 K as compared to B = 835 cm^{-1}, C = 3080 cm^{-1}, Dq = 760 cm^{-1} at 300 K. This indicates that there is no big difference in the absorption spectra of Mn^{2+} at 77 and 300 K. Thus the explanation given above for the calculated results matching equally well at 77 and 300 K seems reasonable.

TABLE IV: Experimental and theoretical energy values of different transitions in Mn^{2+} ion doped DGCCT single crystal.

Transition from $^6A_{1g}(S)$	Observed wave number (cm^{-1})	Calculated wave number (cm^{-1})
$^4T_{1g}(G)$	13889(10)	
	15385(10)	18469(7)
$^4A_{1g}(G)$	19417(9)	19022(75)
$^4E_g(G)$	20833(8)	20834(69)
$^4T_{2g}(G)$	21739(6)	22340(12)
$^4T_{2g}(D)$	23529(5)	22960(10)
$^4E_g(D)$	25157(7)	25187(28)
$^4T_{1g}(P)$	28986(11)	28938(230)
$^4T_{1g}(F)$	32216(12)	32188(142)
$^4A_{2g}(F)$	38986(13)	38659(187)
	40193(15)	40267(160)

V. CONCLUSIONS

The EPR zero field splitting parameters (ZFSPs) have been investigated using the superposition model and perturbation formulae. The experimental ZFSPs obtained for Mn^{2+} ion in DGCCT single crystal are in reasonable agreement with the calculated ZFSPs at the substitutional site. The calculated optical spectra are in reasonable agreement with the experimental ones. We suggest that the Mn^{2+} ion occupies a substitutional Ca^{2+} site in DGCCT. The results support the inference drawn from the experimental data.

Acknowledgement

The authors are thankful to Prof. C. Rudowicz, Molecular Spectroscopy Group, Szecin University of Technology, Poland for providing the CFA program for calculating optical spectra. One of the authors, Sangita Pandey is thankful to the Head, Department of Physics, University of Allahabad for providing the facilities of the department.

APPENDIX A

Relations for the CFPs derived within the superposition model for the Mn^{2+} ion positioned at the substitutional site in DGCCT single crystal:

$$\begin{aligned} B_{20} &= \overline{A_2}(R_0)[(R_0/R_1)^{t_2}(3\cos^2\theta_1 - 1) + (R_0/R_1')^{t_2}(3\cos^2\theta_1' - 1) \\ &\quad +(R_0/R_2)^{t_2}(3\cos^2\theta_2 - 1) + (R_0/R_2')^{t_2}(3\cos^2\theta_2' - 1)], \end{aligned} \tag{A1}$$

$$\begin{aligned} B_{22} &= \sqrt{6}\overline{A_2}(R_0)[(R_0/R_1)^{t_2}\sin^2\theta_1\cos(2\phi_1) + (R_0/R_1')^{t_2}\sin^2\theta_1'\cos(2\phi_1') \\ &\quad +(R_0/R_2)^{t_2}\sin^2\theta_2\cos(2\phi_2) + (R_0/R_2')^{t_2}\sin^2\theta_2'\cos(2\phi_2')]/2, \end{aligned} \tag{A2}$$

$$\begin{aligned} B_{40} &= \overline{A_4}(R_0)[(R_0/R_1)^{t_4}(35\cos^4\theta_1 - 30\cos^2\theta_1 + 3) \\ &\quad +(R_0/R_1')^{t_4}(35\cos^4\theta_1' - 30\cos^2\theta_1' + 3) \\ &\quad +(R_0/R_2)^{t_4}(35\cos^4\theta_2 - 30\cos^2\theta_2 + 3) \\ &\quad +(R_0/R_2')^{t_4}(35\cos^4\theta_2' - 30\cos^2\theta_2' + 3)], \end{aligned} \tag{A3}$$

$$\begin{aligned} B_{42} &= \sqrt{10}\overline{A_4}(R_0)[(R_0/R_1)^{t_4}\sin^2\theta_1(7\cos^2\theta_1 - 1)\cos(2\phi_1) \\ &\quad +(R_0/R_1')^{t_4}\sin^2\theta_1'(7\cos^2\theta_1' - 1)\cos(2\phi_1') \\ &\quad +(R_0/R_2)^{t_4}\sin^2\theta_2(7\cos^2\theta_2 - 1)\cos(2\phi_2) \\ &\quad +(R_0/R_2')^{t_4}\sin^2\theta_2'(7\cos^2\theta_2' - 1)\cos(2\phi_2')], \end{aligned} \tag{A4}$$

$$\begin{aligned} B_{44} &= \sqrt{70}\overline{A_4}(R_0)[(R_0/R_1)^{t_4}\sin^4\theta_1\cos(4\phi_1) + (R_0/R_1')^{t_4}\sin^4\theta_1'\cos(4\phi_1') \\ &\quad +(R_0/R_2)^{t_4}\sin^4\theta_2\cos(4\phi_2) + (R_0/R_2')^{t_4}\sin^4\theta_2'\cos(4\phi_2')]/2. \end{aligned} \tag{A5}$$

References

[1] M. I. Bradbury, D. J. Newman, Chem. Phys. Lett. **1**, 44 (1967). doi: 10.1016/0009-2614(67)80063-0
[2] D. J. Newman, J. Phys. C: Solid State Phys. **10**, L315 (1977). doi: 10.1088/0022-3719/10/11/008
[3] E. Siegel and K. A. Müller, Phys. Rev. B **20**, 3587 (1979). doi: 10.1103/PhysRevB.20.3587
[4] Y. Y. Yeung, J. Phys. C: Solid State Phys. **21**, 2453 (1988). doi: 10.1088/0022-3719/21/13/010
[5] T. H. Yeom, S. H. Choh, and M. L. Du, J. Phys.: Condens. Matter **5**, 2017 (1993). doi: 10.1088/0953-8984/5/13/017
[6] M. J. D. Powell, J. R. Gabriel, and D. F. Johnston, Phys. Rev. Lett. **5**, 145 (1960). doi: 10.1103/PhysRevLett.5.145
[7] H. Watnabe, Prog. Theor. Phys. **18**, 405 (1960).
[8] H. Watnabe, Phys. Rev. Lett. **4**, 410 (1960).
[9] J. R. Gabriel, D. F. Johnston, and M. J. D. Powell, Proc. Roy. Soc. **264**, 503 (1961). doi: 10.1098/rspa.1961.0214
[10] W. Low and G. Rosengarten, J. Mol. Spectrosc. **12**, 319 (1964). doi: 10.1016/0022-2852(64)90018-9
[11] M. Sato, A. S. Rispin, and H. Kon, J. Chem. Phys. **18**, 211 (1976).
[12] M. L. Du and M. G. Zhao, J. Phys. C: Solid State Phys. **18**, 3241 (1985).
[13] X. Y. Kuang and Z. H. Chen, Phys. Rev. B **36**, 797 (1987).
[14] W. L. Yu, Phys. Rev. B **39**, 622 (1989). doi: 10.1103/PhysRevB.39.622
[15] M. G. Brik, C. N. Avram, and N. M. Avram, Physica B **384**, 78 (2006).
[16] Z. Y. Yang, J. Phys.: Condens. Matter **12**, 4091 (2000). doi: 10.1088/0953-8984/12/17/314
[17] R. Kripal and M. Bajpai, Chin. J. Phys. **48**, 671 (2010).
[18] W. L. Yu and M. G. Zhao, Phys. Rev. B **37**, 9254 (1988). doi: 10.1103/PhysRevB.37.9254
[19] S. Natarajan and J. K. Mohana Rao, Curr. Sci. **45**, 490 (1976).
[20] A. Abragam and B. Bleaney, *EPR of Transition Ions* (Clarendon Press, Oxford, 1970).
[21] C. Rudowicz, Magn. Reson. Rev. **13**, 1 (1987).
[22] C. Rudowicz and H. W. F. Sung, Physica B **300**, 1 (2001). doi: 10.1016/S0921-4526(01)00568-3
[23] C. J. Radnell, J. R. Pilbrow, S. Subramanian, and M. T. Rogers, J. Chem. Phys. **62**, 4948 (1975). doi: 10.1063/1.430410
[24] J. A. Weil and J. R. Bolton, *Electron Paramagnetic Resonance: Elementary Theory and Practical Applications*, 2nd Edition (Wiley, New York, 2007).
[25] C. Rudowicz and S. B. Madhu, J. Phys.: Condens. Matter **11**, 273 (1999). doi: 10.1088/0953-8984/11/1/022
[26] C. Rudowicz and R. Bramley, J. Chem. Phys. **83**, 5192 (1985); R. Kripal, D. Yadav, C. Rudowicz, and P. Gnutek, J. Phys. Chem. Solids **70**, 827 (2009).
[27] C. Rudowicz, Y. Y. Zhao, and W. L. Yu, J. Phys. Chem. Solids **53**, 1227 (1992). doi: 10.1016/0022-3697(92)90043-D
[28] W. L. Yu and M. G. Zhao, Phys. Stat. Sol. (b) **140**, 203 (1987).
[29] C. K. Jorgensen, *Modern Aspects of Ligand Field Theory* (North-Holland, Amsterdam, 1971) p 305.
[30] M. G. Zhao, M. L. Du, and G. Y. Sen, J. Phys. C: Solid State Phys. **20**, 5557 (1987); Q. Wei, Acta Phys. Polon. **A118,** 670 (2010).
[31] D. J. Newman, Adv. Phys. **20**, 197 (1970).
[32] Y. Y. Yeung and D. J. Newman, Phys. Rev. B **34**, 2258 (1986).
[33] D. J. Newman, D. C. Pryce, and W. A. Runciman, Am. Miner. **63**, 1278 (1978).

[34] G. Y. Shen and M. G. Zhao, Phys. Rev. B **30**, 3691 (1984). doi: 10.1103/PhysRevB.30.3691
[35] D. J. Newman and B. Ng, Rep. Prog. Phys. **52**, 699 (1989). doi: 10.1088/0034-4885/52/6/002
[36] M. Andrut, M. Wildner, and C. Rudowicz, in *Optical Absorption Spectroscopy in Geosciences, Part II* (Quantitative Aspects of Crystal Fields, Spectroscopic Methods in Mineralogy, EMU Notes in Mineralogy, Vol. **6**, Eds. A. Beran and E. Libowitzky (Eötvös University Press, Budapest, 2004), Chapter 4 p. 145.
[37] C. Rudowicz, J. Phys. C: Solid State Phys. **18**, 1415 (1985); **20**, 6033 (1987). doi: 10.1088/0022-3719/20/35/018
[38] M. Karbowiak, C. Rudowicz, and P. Gnutek, Opt. Mater. **33**, 1147 (2011). doi: 10.1016/j.optmat.2011.01.027
[39] K. T. Han and J. Kim, J. Phys.: Condens. Matter **8**, 6759 (1996). doi: 10.1088/0953-8984/8/36/026
[40] P. Gnutek, Z. Y. Yang, and C. Rudowicz, J. Phys.: Condens. Matter **21**, 455402 (2009). doi: 10.1088/0953-8984/21/45/455402
[41] V. V. Laguta *et al.*, Phys. Rev. **B61**, 3897 (2000). doi: 10.1103/PhysRevB.61.3897
[42] C. Rudowicz and Y. Y. Zhou, J. Magn. Magn. Mater. **111**, 153 (1992). doi: 10.1016/0304-8853(92)91070-A
[43] Y. Y. Yeung and D. J. Newman, J. Chem. Phys. **82**, 3747 (1985). doi: 10.1063/1.448911
[44] M. Acikgöz, P. Gnutek, and C. Rudowicz, Chem. Phys. Letts. **524**, 49 (2012).
[45] Y. Y. Yeung and C. Rudowicz, Comput. Chem. **16** 207 (1992); Y. Y. Yeung and C. Rudowicz, J. Comput. Phys. **109**, 150 (1993).
[46] (a) Z. Y. Yang, Y. Hao, C. Rudowicz, and Y. Y. Yeung, J. Phys.: Condens. Matter **16**, 3481 (2004); (b) P. Gnutek, Z. Y. Yang, and C. Rudowicz, J. Phys.: Condens. Matter **21**, 455402 (2009).
[47] A. Mehra and P. Venkateswarlu, J. Chem. Phys. **47**, 2334 (1967). doi: 10.1063/1.1703315